Triple-Quantum Two-Dimensional ^{27}Al Magic-Angle Spinning Nuclear Magnetic Resonance Spectroscopic Study of Aluminosilicate and Aluminate Crystals and Glasses

J. H. Baltisberger,[†] Z. Xu,[‡] J. F. Stebbins,*[,‡] S. H. Wang,[§] and A. Pines[§]

Contribution from the Department of Chemistry, Berea College, Berea, Kentucky 40404, Department of Geological and Environmental Sciences, Stanford University, Stanford, California 94305, and Materials Sciences Division, Lawrence Berkeley Laboratory, 1 Cyclotron Rd., Berkeley, California 94720

Received February 28, 1996[⊗]

Abstract: A new two-dimensional magic-angle spinning NMR experiment[1,2] using multiple-quantum coherences of half-integer quadrupolar nuclei was used to study ^{27}Al sites in crystalline samples of leucite ($KAlSi_2O_6$), anorthite ($CaAl_2Si_2O_8$), and kyanite (Al_2SiO_5), as well as $CaAl_2Si_2O_8$ glass and a magnesium aluminoborate glass. In the crystals, multiple sites are partially resolved and new results for isotropic chemical shifts and quadrupolar parameters are derived, using data collected at a single magnetic field. Data for both leucite and anorthite are consistent with previous results that correlate chemical shifts with mean intertetrahedral bond angle. Signal can be obtained from sites with quadrupolar coupling constants as large as 9 MHz, but intensities are reduced. In the aluminoborate glass, peaks for sites with different Al coordination numbers are well separated. The lack of such features in $CaAl_2Si_2O_8$ glass rules out the presence of significant quantities of AlO_5 and AlO_6 groups.

Introduction

Aluminum-containing oxide crystals and glasses are abundant in nature as well as being among the most commonly used technological materials. Understanding the structures of these materials is thus fundamental to many problems in earth and in materials sciences. High resolution solid-state NMR is becoming increasingly important in resolving such problems, particularly in quantifying the extent and nature of disorder. ^{27}Al NMR holds great potential, but results from simple MAS spectra have been limited by the low resolution generally caused by second-order quadrupolar broadening. Several approaches have been taken to eliminate or reduce such effects, including dynamic angle spinning (DAS),[3−8] double rotation (DOR),[7−9] and the observation of spinning sidebands for satellite transitions,[10−12] although DAS NMR has generally been unfeasible for ^{27}Al because of short spin−lattice relaxation times and strong homonuclear dipolar couplings.

The most recent development in this effort has been to exploit multiple quantum coherences in two-dimensional MAS experiments ("MQMAS").[13] Double-quantum spectra under magic angle spinning conditions were previously observed for ^{2}H in solids.[14] A version of this experiment, involving triple quantum coherence ("3QMAS"), has been documented as being particularly effective for spin $^3/_2$ nuclides such as ^{23}Na and ^{87}Rb, as well as for spin $^5/_2$ ^{27}Al.[1,2,15,16] Applications of this new approach, to complex, multisite crystals and to amorphous materials, have been very limited thus far, however. Very recently, the analogous five-quantum experiment has been found useful for enhancing resolution for ^{27}Al in aluminophosphate molecular sieve materials.[17] In this paper we explore the utility, and the limitations, of the two-dimensional, triple-quantum MAS experiment in several crystalline aluminosilicates and in several alumina-rich oxide glasses. We show that the additional information in a 2D 3QMAS experiment may be used to extract quadrupolar parameters and isotropic chemical shifts. In favorable cases, at least, such information can thus be obtained without acquiring spectra at a second magnetic field and without additional NMR experiments.

* To whom correspondance should be addressed.
† Berea College.
‡ Stanford University.
§ Lawrence Berkeley Laboratory.
⊗ Abstract published in *Advance ACS Abstracts,* July 15, 1996.

(1) Frydman, L.; Harwood, J. S. *J. Am. Chem. Soc.* **1995**, *117,* 5367−5368.
(2) Massiot, D.; Touzo, B.; Trumeau, D.; Coutures, J. P.; Virlet, J.; Florian, P.; Grandinetti, P. J. *Solid State NMR* **1996**, *6,* 73−84.
(3) Baltisberger, J. H.; Gann, S. L.; Wooten, E. W.; Chang, T. H.; Mueller, K. T.; Pines, A. *J. Am. Chem. Soc.* **1992**, *114,* 7489−7493.
(4) Grandinetti, P. J.; Lee, Y. K.; Baltisberger, J. H.; Sun, B. Q.; Pines, A. *J. Magn. Reson. A* **1993**, *103,* 195−204.
(5) Mueller, K. T.; Sun, B. Q.; Chingas, C. G.; Zwanziger, J. W.; Terao, T.; Pines, A. *J. Magn. Reson.* **1990**, *86,* 470−487.
(6) Mueller, K. T.; Wooten, E. W.; Pines, A. *J. Mag. Reson.* **1991**, *92,* 620−627.
(7) Sun, B. Q.; Baltisberger, J. H.; Wu, Y.; Samoson, A.; Pines, A. *Solid State NMR* **1992**, *1,* 267−295.
(8) Wu, Y.; Sun, B. Q.; Pines, A.; Samoson, A.; Lippmaa, E. *J. Magn. Reson.* **1990**, *89,* 297−309.
(9) Jelinek, R.; Chmelka, B. F.; Wu, Y.; Grandinetti, P. J.; Pines, A.; Barrie, P. J.; Klinowski, J. *J. Am. Chem. Soc.* **1991**, *113,* 4097−4101.
(10) Jäger, C.; Kunath, G.; Losso, P.; Scheler, G. *Solid State Nucl. Magn. Reson.* **1993**, *2,* 73−82.
(11) Skibsted, J.; Nielsen, N. C.; Bildsøe, H.; Jakobsen, H. J. *J. Magn. Reson.* **1991**, *95,* 88−117.
(12) Jakobsen, H. J.; Skibsted, J.; Bildsøe, H.; Nielsen, N. C. *J. Magn. Reson.* **1989**, *85,* 173−180.
(13) Emsley, L.; Pines, A. in *Lectures on pulsed NMR,* 2nd ed.; Maraviglia, B., Ed.; Societa Italiana di Fisica, 1994; pp 1−266.
(14) Müller, L.; Eckman, R.; Pines, A. *Chem. Phys. Lett.* **1980**, *74,* 376−378.
(15) Medek, A.; Harwood, J. S.; Frydman, L. *J. Am. Chem. Soc.* **1995**, *117,* 12779−12787.
(16) Fernandez, C.; Amoureuz, J. P. *Solid State NMR* **1996**, *5,* 315−321.
(17) Fernandez, C.; Amoureux, J. P. *Chem. Phys. Lett.* **1995**, *242,* 449−454.

S0002-7863(96)00658-0 CCC: $12.00

Theory

The theory of 3QMAS has been previously presented in the literature and will not be extensively reviewed here.[1,2] The fundamental concept in second-order averaging techniques (DAS, DOR, MQMAS) is that additional degrees of freedom need to be brought to bear on the quadrupolar interaction. In DAS and DOR the additional degree of freedom comes in rendering the spinning angle time dependent. This time dependence is exploited to remove both the P_2 and P_4 (second and fourth rank spatial tensors) dependent terms in the Hamiltonian. In the MQMAS experiment, the degree of freedom that is beneficially manipulated is coherence order. Normally, half-odd integer quadrupolar nuclei are studied using a $p = \pm 1$ coherence (corresponding to $m = {}^1/_2 \leftrightarrow -{}^1/_2$ transition). For MQMAS the $p = \pm 3$ or ± 5 coherences are used as a second degree of freedom. Since evolution frequency has different spatial dependences under different coherence orders, it is possible to average the second rank terms with the rapid sample spinning and the fourth rank terms with multiple quantum coherence mixing. Note that *both* second- *and* fourth-order spatial terms cannot be averaged simultaneously using *only* multiple quantum coherences, that is to say spinning is essential.

Experimental Methods

Samples. The sample of the natural framework silicate mineral leucite ($KAlSi_2O_6$, from the Roman volcanic province) has been previously studied in detail by ^{29}Si MAS NMR.[18] Several samples of crystalline anorthite ($CaAl_2Si_2O_8$, also a framework silicate) were prepared by the method described in a detailed study of Si/Al disorder.[19] A glass of this composition was prepared by melting the constituent oxides at 1650 °C for about 1 h followed by air quenching. Several portions of the glass were then crystallized by annealing at 1400 °C for either 4 min (sample 1) or 65 h (sample 2). Powder X-ray diffraction and ^{29}Si MAS NMR spectra on these samples showed only anorthite to be present. ^{29}Si MAS NMR spectra closely resemble those of Phillips et al.[19] for samples crystallized for 15 min and 179 h, respectively, and thus have a smaller difference in the extent of disorder than expected (presumably because of vagaries of thermal history and nucleation kinetics). A sample of natural kyanite (Al_2SiO_5, locality unknown) was also selected in order to test the relative excitation efficiencies for Al sites with widely varying quadrupolar coupling constants. A glass of composition 40 mole % MgO, 40 mol % B_2O_3, and 20 mol % Al_2O_3 was selected because of its large concentrations of 4-, 5-, and 6-coordinated Al as determined previously by ^{27}Al MAS NMR,[20,21] and was also prepared by standard mixing and melting of the oxides.

NMR Spectroscopy. The MAS experiments at 9.4 T were performed on a modified Varian VXR-400S spectrometer with a 5-mm high-speed MAS probe from Doty Scientific, Inc., with spinning rates of about 11 kHz. At 11.7 T, experiments were performed on a Chemagnetics spectrometer using the same probe. In order to assure that relative peak intensities were not affected by differential spin−lattice relaxation rates, spectra were acquired with varying delay times between pulses in preliminary MAS experiments. No variations in peak shapes were observed. Spin−lattice relaxation times (T_1) were measured with the saturation-recovery method, and delay times in 3QMAS experiments were chosen to be at least 3 times T_1 to assure nearly complete relaxation. The low efficiency of the triple quantum excitation and the two-dimensional data acquisition resulted in typical total acquisition times for the spectra shown here of 24 h, much longer than times typically required for 1D, single quantum MAS experiments (typically a few minutes for ^{27}Al). Useful 3QMAS spectra can generally be obtained in somewhat shorter times of a few hours.

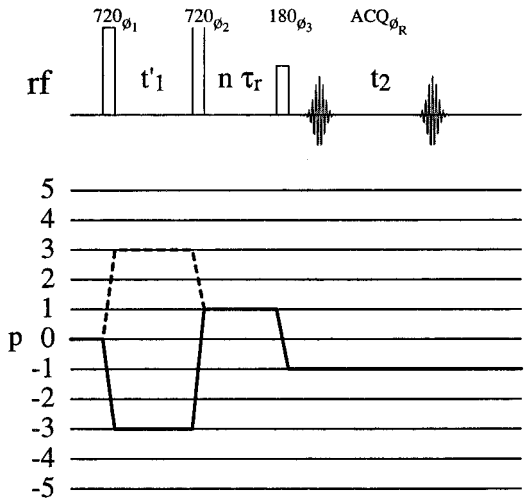

Figure 1. Pulse sequence used for acquisition of pure absorption phase 2D 3QMAS spectra (top) and coherence pathway used to achieve pure phase (bottom). Note that the ±3 coherences are separated in a hypercomplex fashion.[2]

The pulse sequence used was the 3QMAS echo sequence described previously[2] and shown in Figure 1. The first and second pulses of this sequence are hard (ideally nonselective) 360° or 720° pulses (that is they are applied with the highest allowable power). In our case, this required pulses of 15−20 μs. The third pulse was a soft (central transition selective) pulse of 180° which was approximately 15−20 μs in duration as well. The delay between the first and second pulses was the t_1 period which was selected to have a dwell time equal to the desired t_1 dwell time (after complete processing) multiplied by 12/31. This factor arises as the 3QMAS experiment for a spin $^5/_2$ nucleus is mathematically equivalent to a $k = 19/12$ DAS experiment.[5] In our experiments the MAS t_2 spectral width was usually 6−20 kHz while in the t_1 dimension it was usually 6−15 kHz. A 10 kHz t_1 dimension spectral width required the actual t_1 dwell time to be set to 38.7 μs. In these experiments, usually 40−100 t_1 points were required to obtain spectra without truncation artifacts. The delay between the second and third pulses was set to an integer multiple of the period of the spinning rate, τ_r. This is required to ensure that the echo is completely refocused and no additional rotational artifacts are introduced. Care must be taken, just as in a shifted-echo DAS (SEDAS) experiment, to set the echo time to an appropriate value. If it is too long, then too much signal is lost; if it is too short, then the data will be truncated in the t_2 dimension (remembering that whole echo in this dimension is collected). Details on setting this delay in general are discussed elsewhere;[2,22] for our experiments it was set to values ranging from 1 to 3 ms (10−30 rotor cycles). The spinning sidebands appear in positions similar to those that would be predicted from a $k = 19/12$ DAS experiment and the processing is identical as well.[2,4−7,22] The only difference arises in the referencing stage, at which point the offset in the isotropic dimension (the ppm value of the center of the resulting t_1 dimension spectrum) must be multiplied by $(k - 3)/(k + 1)$ or $-17/31$.[2]

The determination of the isotropic chemical shift (δ_{iso}^{cs}) and quadrupolar coupling product P_q ($C_q(1 + \eta^2/3)^{1/2}$ where $C_q = e^2qQ/h$ and η is the quadrupolar asymmetry parameter) was similar to that performed in a multiple field DAS experiment, in which the isotropic shift changes with field due to the differing second-order isotropic quadrupolar shift ($\delta_{iso}^{2Q} = (6 \times 10^{-3})P_q^2/\nu_0^2$).[3,23] In the 3QMAS experiment, the isotropic shift has scaling factors that differ from those of a single quantum spectrum. Thus the separation of δ_{iso}^{cs} and δ_{iso}^{2Q} can be made with a single experiment at a single field. For $I = {}^5/_2$, the observed

(18) Murdoch, J. B.; Stebbins, J. F.; Carmichael, I. S. E.; Pines, A. *Phys. Chem. Miner.* **1988**, *15*, 370−382.

(19) Phillips, B. L.; Kirkpatrick, R. J.; Carpenter, M. A. *Am. Miner.* **1992**, *77*, 484−495.

(20) Bunker, B. C.; Kirkpatrick, R. J.; Brow, R. K. *J. Am. Ceram. Soc.* **1991**, *74*, 1425−1429.

(21) Bunker, B. C.; Kirkpatrick, R. J.; Brow, R. K.; Turner, G. L.; Nelson, C. *J. Am. Ceram. Soc.* **1991**, *74*, 1430−1438.

(22) Grandinetti, P. J.; Baltisberger, J. H.; Llor, A.; Lee, Y. K.; Werner, U.; Eastman, M. A.; Pines, A. *J. Magn. Reson. A* **1993**, *103*, 72−81.

(23) Mueller, K. T.; Baltisberger, J. H.; Wooten, E. W.; Pines, A. *J. Phys. Chem.* **1992**, *96*, 7001−7004.

Table 1. Isotropic Shifts and Quadrupolar Coupling Parameters for Leucite from 11.7 and 9.4 T 3QMAS Experiments, Derived from 3QMAS and MAS Peak Positions[a]

site	$\delta_{MAS}^{9.4T}$ (ppm)	$\delta_{3QMAS}^{9.4T}$	$\delta_{MAS}^{11.7T}$	$\delta_{3QMAS}^{11.7T}$	δ_{iso}^{cs}	P_q (MHz)
T1	58.6 ± 2.0	-34.2 ± 0.2	59.6 ± 1.5	-34.0 ± 0.2	61.0 ± 0.7	2.07 ± 0.50
T2	59.7 ± 2.0	-36.4 ± 0.2	61.8 ± 1.5	-35.7 ± 0.2	63.9 ± 0.6	2.58 ± 0.50
T3	66.1 ± 2.0	-39.1 ± 0.2	67.2 ± 1.5	-38.4 ± 0.2	69.2 ± 0.7	2.34 ± 0.50

[a] Peak assignments are based on correlations between chemical shift and mean T−O−T bond angles.[29] P_q is the quadrupolar product, $C_q(1 + \eta^2/3)^{1/2}$.

peak position in the ω_1 (triple quantum) dimension can be described as:[2]

$$\delta_{3QMAS} = -(17/31)\delta_{iso}^{cs} + (10/31)\delta_{iso}^{2Q}$$

The center of gravity of the same peak in the ω_2 (MAS) dimension is:

$$\delta_{MAS} = \delta_{iso}^{cs} + \delta_{iso}^{2Q}$$

The values of δ_{iso}^{cs} and δ_{iso}^{2Q} (or P_q) can thus be extracted by combining data from both dimensions.

In the second approach, MAS peak shapes in slices of the 2D spectra were fitted with a least-squares program (utilizing the CERN MINUIT routines) in which all relevant parameters in the MAS peak shape (C_q, η, δ_{iso}^{cs}, integrated intensity, Lorentzian and Gaussian broadening) were allowed to vary. In general, the two methods produced similar results, although the latter approach may allow η and C_q to be derived in addition to P_q.

Results

Leucite. Leucite has a complex structure with three crystallographically distinct tetrahedral sites (T_1, T_2, T_3). Because of the complexity of the ^{29}Si spectrum (as many as 15 overlapping peaks) and the low resolution of the ^{27}Al MAS spectrum, the fraction of the total Al on each site remains imprecisely known. Models of essentially identical ^{29}Si spectra have yielded fractions of about 0.4, 0.2, and 0.4 on T_1, T_2, and T_3, respectively, in one model,[18] 0.25, 0.50, and 0.25 in a second model,[24] and 0.50, 0.25, and 0.25 in a third.[25] In contrast, analysis of ^{27}Al MAS data suggested fractions of 0.50, 0.25, and 0.25.[26]

The ^{27}Al 2D 3QMAS spectrum of leucite (Figure 2) shows three partially overlapping peaks corresponding to the three sites. The projection in the isotropic dimension shows considerably better resolution than MAS spectra collected at 11.7 T and lower fields.[24−26] Although three partially resolved peaks were observed in the spinning sidebands for the $\pm^1/_2{-}^3/_2$ transitions,[26] the 3QMAS data are more definitive in ruling out any influence of second order quadrupolar coupling on peak shape. Fitting the projection with three Gaussian peaks suggests that the intensities of the three peaks are equal within about a ±20% error. Residual broadening, presumably due to the disordered arrangement of second-neighbor cations and a resulting distribution of isotropic chemical and quadrupolar shifts, appears to limit the ultimate resolution.

Imperfect, site-dependent excitation has the potential to be quite significant in 3QMAS experiments, making quantitation of intensities complex. The excitation from equilibrium (zero-quantum) to a triple-quantum coherence is a forbidden transition in a first-order approximation. A more thorough examination of the Hamiltonians shows that a long pulse is capable of transferring coherence from a zero to a triple quantum state.[1,14,15] The efficiency of this process is highly dependent on C_q and on the overall RF field strength. An assumption of uniform excitation is thus most likely to be valid if C_q values for different sites are similar. Exact C_q values are not known for leucite, but data for isotropic chemical shifts and for P_q can be extracted from the 2-dimensional 3QMAS spectra as described above. Results are shown in Table 1. Chemical shifts agree well with values previously derived from MAS spectra including satellite sidebands, and P_q data are consistent with previous rough estimates of 1−2 MHz.[26] The close similarity of the P_q values for the three peaks suggests that in this case intensities in the 3QMAS experiment are likely to be quantitative and thus imply site occupancies that are somewhat discrepant from previous models. Given the disagreements among existing models, however, the significance of their differences with the present data is uncertain.

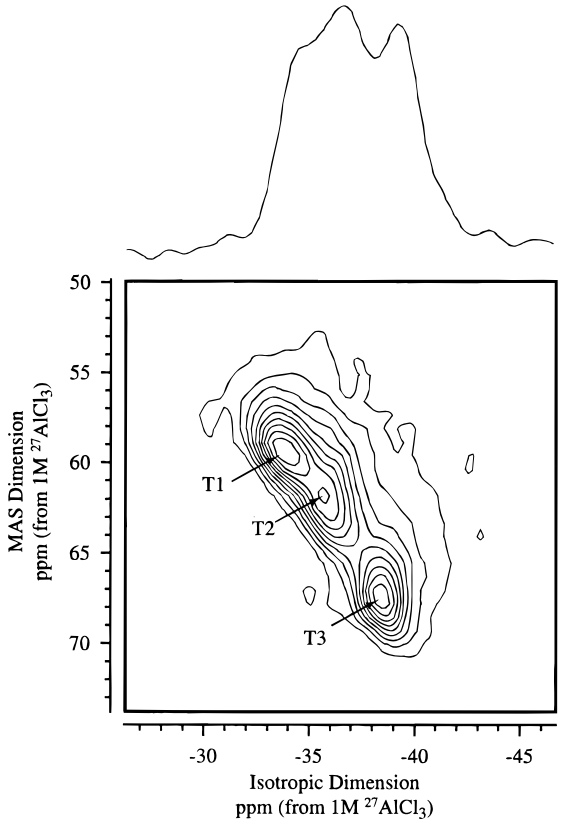

Figure 2. Contour plot of the ^{27}Al 3QMAS NMR spectrum for leucite at 11.7 T. The contour lines are at levels from 5 to 90% in 9.4% steps. The 1D spectrum on top is the projection onto the isotropic dimension.

Kyanite. Kyanite was studied to further assess the quantitation of 3QMAS peak intensities. The mineral contains four equally populated octahedral Al sites, with C_q values of 10.0, 9.4, 6.5, and 3.7 MHz.[27] The MAS spectrum is contrasted with the isotropic projection of the 3QMAS spectrum in Figure 3. The resolution in the latter is dramatically increased: separation of the peaks in the latter is enhanced by the large range in C_q, and peaks are much narrower because of the full averaging of

(24) Kohn, S. C.; Henderson, C. M. B.; Dupree, R. *Am. Miner.* **1995**, *80*, 705−714.
(25) Brown, I. W. M.; Cardile, C. M.; MacKenzie, K. J. D.; Ryan, M. J.; Meinhold, R. H. *Phys. Chem. Miner.* **1987**, *15*, 78−83.
(26) Phillips, B. L.; Kirkpatrick, R. J.; Putnis, A. *Phys. Chem. Miner.* **1989**, *16*, 591−598.
(27) Stebbins, J. F. In *Nuclear magnetic resonance spectroscopy of silicates and oxides in geochemistry and geophysics*; Ahrens, T. J., Ed.; American Geophysical Union: Washington DC, 1995; pp 303−332.

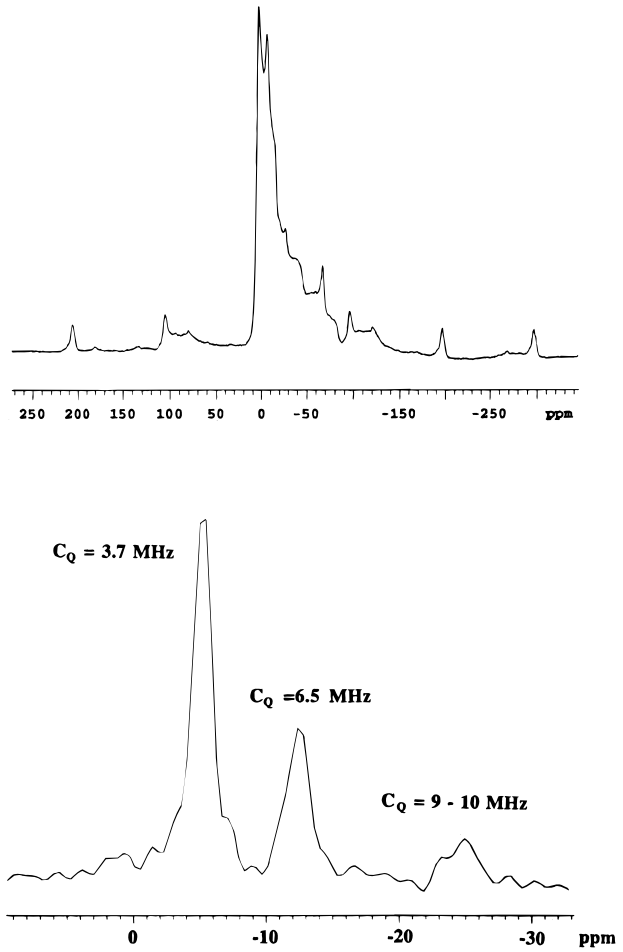

Figure 3. (Top) ^{27}Al MAS spectrum for kyanite; (bottom) isotropic projection of the 3QMAS spectrum at 9.4 T.

the second-order quadrupolar broadening. Even sites with very large C_q values are excited and observed. However, it is clear that observed intensities are systematically reduced with increasing C_q, suggesting that caution is required in materials where ranges of C_q are large or unknown.

Crystalline Anorthite. Anorthite is an excellent test for ^{27}Al spectral resolution: it has eight crystallographically distinct tetrahedral Al sites and is fully ordered (natural samples) or nearly so (synthetic samples). C_q and η values for all sites have been reported from single crystal data,[28] but isotropic chemical shifts are not known because ^{27}Al MAS spectra are completely unresolved.

3QMAS data at 11.7 T for more ordered crystalline anorthite are shown in Figure 4 (the spectrum at 9.4 T is available in supporting information). The spectra are complex, but contain a number of significant, resolvable features. The spectra were essentially the same in overall appearance with slight shifts between the two fields. Results for the somewhat less ordered crystal are very similar, if perhaps slightly less well-resolved, and have not been analyzed in detail. We have taken two independent approaches to understanding the spectra. In both, slices through the 2D spectra at the positions of obvious spectral features were taken (Figure 4). In the first approach, the peak position in the ω_1 dimension (δ_{3QMAS}) and the center of gravity in the ω_2 (MAS) dimension were determined, and δ_{iso}^{cs} and P_q were calculated directly as described above. Results for the two fields are shown in Tables 2 and 3, and are consistent with each other within estimated uncertainties.

MAS peak shapes in slices of the 2D spectra were also simulated as described in the Experimental Section. For

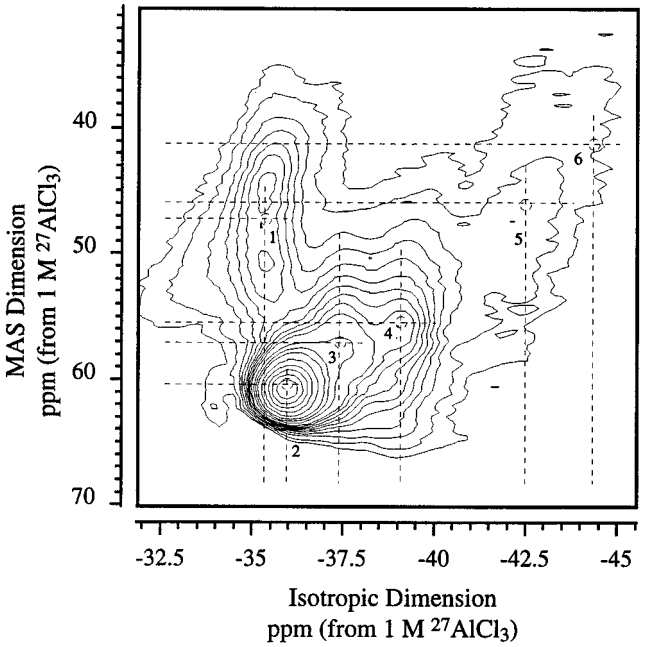

Figure 4. Contour plot of the ^{27}Al 3QMAS NMR spectrum for anorthite at 11.7 T. The contour lines are drawn at levels from 2 to 24% in 2% increments and in 10% increments from 30 to 90%. Numbered points show the positions of singularities, through which slices were taken for simulation and calculation of δ_{iso}^{cs}, P_q, and C_q.

Table 2. Isotropic Shifts and Quadrupolar Coupling Parameters for Crystalline Anorthite from 11.7 T 3QMAS Experiments, Derived from 3QMAS and MAS Peak Positions

peak	$\delta_{MAS}^{11.7T}$ (ppm)	$\delta_{3QMAS}^{11.7T}$ (ppm)	δ_{iso}^{cs} (ppm)	$\mathbf{P}_q$ (MHz)
1	48.0 ± 3.0	−35.4 ± 0.2	58.4 ± 1.1	5.43 ± 0.50
2	61.0 ± 1.0	−36.0 ± 0.2	63.9 ± 0.4	2.88 ± 0.33
3	58.0 ± 3.0	−37.4 ± 0.2	64.4 ± 1.1	4.26 ± 0.63
4	55.0 ± 3.0	−39.1 ± 0.2	65.2 ± 1.1	5.38 ± 0.50
5	47.0 ± 3.0	−42.5 ± 0.2	66.2 ± 1.1	7.37 ± 0.37
6	40.0 ± 5.0	−44.4 ± 0.2	65.8 ± 1.9	8.54 ± 0.52

Table 3. Isotropic Shifts and Quadrupolar Coupling Parameters for Crystalline Anorthite from 9.4 T 3QMAS Experiments Derived from 3QMAS and MAS Peak Positions

peak	$\delta_{MAS}^{9.4T}$ (ppm)	$\delta_{3QMAS}^{9.4T}$ (ppm)	δ_{iso}^{cs} (ppm)	P_q (MHz)
1	40.8 ± 2.0	−37.1 ± 0.3	57.7 ± 0.8	5.53 ± 0.21
2	59.0 ± 1.0	−36.2 ± 0.2	63.4 ± 0.4	2.83 ± 0.20
3	56.0 ± 2.0	−37.1 ± 0.3	63.3 ± 0.8	3.64 ± 0.32
4	51.1 ± 3.0	−39.1 ± 0.3	63.8 ± 1.1	4.80 ± 0.36
5	36.6 ± 4.0	−45.6 ± 0.3	65.9 ± 1.5	7.28 ± 0.32
6	25.0 ± 5.0	−49.0 ± 0.3	65.5 ± 1.9	8.56 ± 0.33

example, the slice projected from −35.5 to −36.5 ppm in the ω_1 dimension (which contains two distinct sites) is shown in Figure 5. The simulated spectrum agrees well, with all singularities appearing in the ω_2 dimension of the experimental data as expected. One possible limitation of such fitting is distortion of the ω_2 dimension (MAS) peak shape due to nonuniform excitation of nuclei in crystallites with different orientation.[15] Results of simulations are shown in Table 4. Fits were checked independently by using the derived parameters to calculate the expected ω_1 peak positions (δ_{3QMAS}). The latter agree well with directly observed values, suggesting that the fits are robust. The simulations provide values for η as well as for C_q and δ_{iso}^{cs}. This procedure allows assignment of at least five features in the spectra to particular crystallographic sites, based on published single crystal data (Table 4). A sixth feature (#6 in Figure 4), at the extreme low-frequency side in ω_1, can be simulated with parameters that are closest to those expected for the 0*zi*0 site (C_q = 8.5 MHz), but could probably also be

(28) Staehli, J. L.; Brinkmann, D. *Z. Kristallogr.* **1974**, *140*, 374−392.

Table 4. Results[a] from Fitting the MAS Projections (Slices) Out of the 3QMAS NMR Spectrum at 11.7 T for Crystalline Anorthite, Compared with Previous Results from Single Crystal NMR[28] and with Mean Si−O−Al Bond Angles from the X-ray Diffraction Structure[31]

		simulation results					single crystal				
peak	δ^{obs}_{3QMAS} (ppm)	δ^{pred}_{3QMAS} (ppm)	δ^{cs}_{iso} (ppm)	C_q (MHz)	η	P_q (MHz)	C_q (MHz)	η	P_q (MHz)	site	mean angle (deg)
1	−35.3	−37.2	60.6	5.76	0.45	5.95	5.5	0.42	5.7	*m*0*i*0	145.4
2	−35.9	−35.8	63.6	2.66	0.53	2.78	2.6	0.66	2.8	*mzi*0	137.9
3	−37.3	−37.9	64.7	4.39	0.51	4.58	4.4	0.53	4.6	0000	138.0
4	−39.1	−39.0	65.6	4.87	0.62	5.17	4.9	0.75	5.3	*mz*00	133.5
5	−42.2	−40.3	66.3	6.58	0.70	7.10	6.8	0.65	7.3	00*i*0	131.1
6	−44.0	−45.0	66.2	8.19	0.65	8.75	8.5	0.66	9.1	0*zi*0	132.0

[a] Uncertainties in fitted C_q values are about ±0.5 MHz; in η about ±0.2, and in δ^{cs}_{iso} about ±1 to 2 ppm.

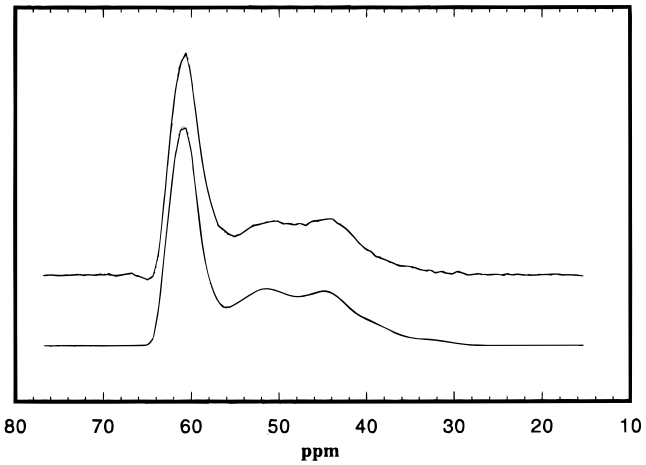

Figure 5. MAS projection from −34.5 to −36.5 ppm in the isotropic dimension of the 11.7 T 3QMAS spectrum of anorthite. The simulation of this slice was fit and the parameters are those for peaks 1 and 2 as shown in Table 4.

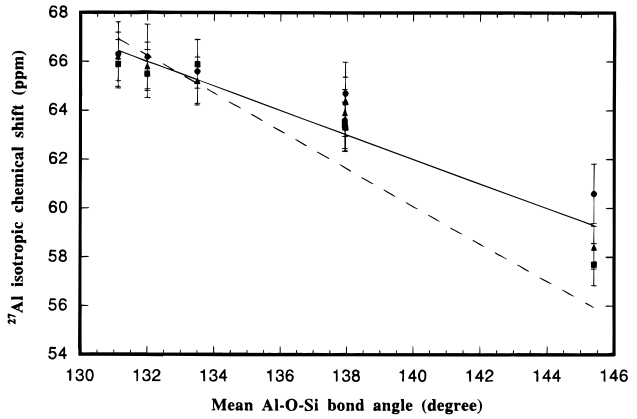

Figure 6. Isotropic chemical shifts for anorthite, derived from 3QMAS data, plotted against the mean Si−O−Al angle (θ) at each site. Only six sites are plotted, as data for the remaining two are not well constrained by the spectra. Solid circles: results from simulations of slices in the 11.7 T spectrum. Solid triangles: results from 2D peak positions at 11.7 T. Solid squares: results from 2D peak positions at 9.4 T. The solid line is a fit to data for a variety of aluminosilicates (both ordered and disordered)[30] with $\delta = -0.50\theta + 132$; the dashed line is a fit to data for ordered structures only,[26] with $\delta = -0.77\theta + 167.9$.

attributed to 0*z*00 ($C_q = 7.4$ MHz) or to *m*000 ($C_q = 6.3$ MHz). In fact, the whole "tail" of the spectrum in this region could well be comprised of poorly resolved signal from the three peaks with largest C_q. As noted above for kyanite, peaks for sites with relatively large C_q are expected to have reduced intensities as well as greater width in the ω_2 dimension, and thus are expected to be relatively difficult to observe with 3QMAS. The broad feature on the high-frequency (ω_1) side of the tallest peak is also likely to be due to an unresolved peak, again possibly one of the unassigned peaks with large C_q. In general, the agreement between the results for δ^{cs}_{iso} and P_q of the two approaches to assigning spectral features is excellent.

The estimated isotropic chemical shifts for the six relatively well-constrained sites are plotted in Figure 6 as a function of the mean intertetrahedral (Si−O−Al) angle. As expected from previous MAS NMR studies of both ^{29}Si and ^{27}Al in framework aluminosilicates,[29] δ^{cs}_{iso} decreases systematically with increasing mean angle. The 3QMAS data fall close to a line previously fitted to data from ordered phases,[29] confirming the accuracy of the new data and of the site assignments. An earlier fit that included data for disordered minerals as well[29,30] agrees even more closely with the anorthite data. The agreement may be fortuitous, in that bond angle calculations for disordered crystals are based on average long-range structure, and thus may be distorted by the lack of data on true local bonding geometry.

$CaAl_2Si_2O_8$ Glass. The 3QMAS spectrum for the glass of anorthite composition is shown in Figure 7, and is broad and unresolved. The peak maximum and the "center of mass" are shifted by roughly 5 ppm from those of the crystal in both dimensions, suggesting a decrease in the mean chemical shift and/or an increase in the mean C_q. The much greater overall width is not surprising in light of the disorder in the glass.

In MAS spectra of glasses in which Al is expected to be four-coordinated by oxygen (as in this composition), there is often significant spectral intensity in the region of isotropic chemical shifts for five- and six-coordinated Al. In the absence of clear, discrete peaks in such spectra, it is generally assumed that such low-frequency "tails" are the result of second-order quadrupolar broadening, and are not due to a distribution of chemical shifts. This assumption is supported by the narrowness of satellite transition sidebands in MAS spectra, and is confirmed strongly by the 2D 3QMAS spectrum: in comparison with clearly separated features for AlO_5 and AlO_6 groups as seen in the glass described below (Figure 8), there is no detectable intensity at the corresponding positions in the $CaAl_2Si_2O_8$ glass. On the other hand, the 2D shapes of the AlO_4 peaks in both glasses are surprisingly similar, perhaps suggesting similar ranges of δ^{cs}_{iso} and C_q.

Magnesium Aluminoborate Glass. This material was chosen because it contains sub-equal concentrations of four-, five-, and six-coordinated Al, which are clearly seen as partially resolved peaks in ^{27}Al MAS NMR spectra.[20,21] The 3QMAS spectrum is shown in Figure 8, and has three well-separated peaks that can be assigned to the three coordinations. The lack of significant overlap of the 2D peaks indicates that 3QMAS NMR may be especially useful for detecting (or excluding) the presence of relatively small concentrations of the higher coordination states, whose presence is likely to be ambiguous in MAS spectra. Estimates of isotropic chemical shifts and quadrupolar products P_q for the the three AlO_n peaks can be

(29) Phillips, B. L.; Kirkpatrick, R. J. *Am. Miner.* **1994**, *79*, 1025−1036.
(30) Lippmaa, E.; Samoson, A.; Mägi, M. *J. Am. Chem. Soc.* **1986**, *108*, 1730−1735.
(31) Wainwright, J. E.; Starkey, J. *Z. Kristallogr.* **1971**, *133*, 75−84.

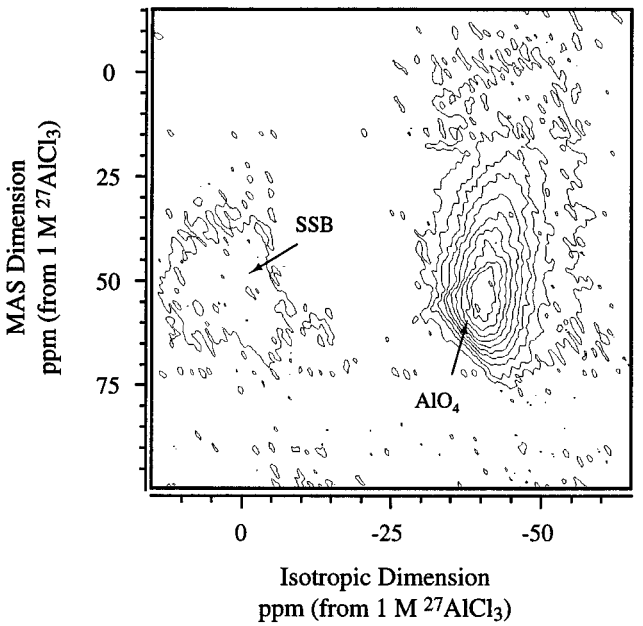

Figure 7. Contour plot of the ^{27}Al 3QMAS NMR spectrum for $CaAl_2Si_2O_8$ (anorthite composition) glass at 11.7 T. The contour lines are drawn at levels from 5 to 90% in 9.4% increments. The peak assignable to AlO_4 sites is labeled. Note the absence of peaks at the AlO_5 and AlO_6 regions seen in Figure 8. The low-intensity feature to the left of the main peak is a spinning sideband (SSB).

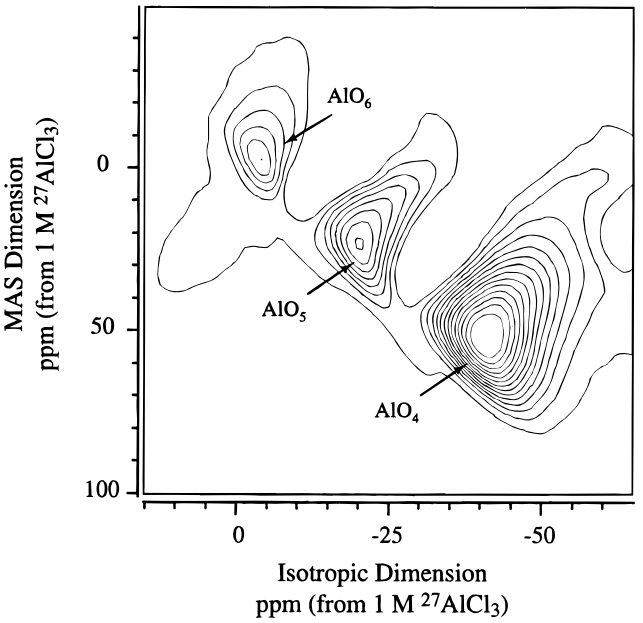

Figure 8. Contour plot of the ^{27}Al 3QMAS NMR spectrum for a glass of composition 40 mol % MgO, 40 mol % B_2O_3, and 20 mol % Al_2O_3 at 9.4 T. The contour lines are drawn at levels from 3 to 90% in 6.7% steps. Peaks assignable to AlO_6, AlO_5, and AlO_4 groups are labeled.

made by measuring the positions of the peak maxima in both dimensions as described above. For the AlO_6, AlO_5, and AlO_4 peaks respectively we obtain 4, 31, and 63 ppm for δ_{iso}^{cs} and 2, 3, and 5 MHz for P_q. These results are complicated by the likelihood of overlap of signal from sites with varying parameters within each major peak, and uncertainties are at least 2 ppm and 0.5 to 1.0 MHz. The relative population of the AlO_6, AlO_5, and AlO_4 sites obtained from the total projection of the 2D spectrum is about 1:2:6. As shown before for the kyanite sample, however, the triple-quantum excitation efficiency for Al sites systematically decreases with increasing P_q. Thus, the intensity observed for the AlO_4 peak is likely to be underestimated relative to the others.

The 2D spectrum is consistent with ranges of chemical shifts and coupling constants known from crystalline materials. AlO_6 sites generally have δ_{iso}^{cs} between 1 and 15 ppm and C_q between 1 and 10 MHz. Corresponding 3QMAS peak positions of -1 to -30 ppm in the isotropic dimension and -50 to 12 ppm in the MAS dimension would be expected. Values of δ_{iso}^{cs} for AlO_5 sites typically fall between 30 and 40 ppm, with C_q between 3 and 10 MHz, giving 3QMAS peak positions ranging from -18 to -40 ppm in the isotropic dimension and -30 to 30 ppm in the MAS dimension. Finally, AlO_4 sites typically have δ_{iso}^{cs} between 55 and 88 ppm and C_q between 1 and 10 MHz, resulting in 3QMAS peak positions from -30 to -60 ppm in the isotropic dimension and 0 to 80 ppm in the MAS dimension. Note that in Figure 8, each of the labeled peaks falls neatly in the center of the corresponding regions.

For the AlO_4 peak we also fitted slices along the ω_2 dimension, as was done for the crystalline phases. Again, for a disordered material results from the fits are not unique because each slice contains unresolved intensity from sites with ranges in chemical shift and C_q. However, this approach does give some estimate of the range of parameters present, about 62 to 75 ppm for δ_{iso}^{cs} and 4 to 6.5 MHz for C_q.

Conclusions

Triple-quantum magic angle spinning (3QMAS) spectra can provide enhanced resolution for ^{27}Al in aluminosilicate and aluminate materials, both crystalline and amorphous, although resolution in the isotropic dimension may still be limited by disorder and other mechanisms of residual broadening. Additional information on NMR parameters may be obtainable because the two dimensional spectra provide some separation of chemical shift and quadrupolar effects, both from simple peak position data and from fitting of MAS peak shapes in slices of the spectra. 3QMAS signal can be obtained even from sites with quadrupolar coupling constants as large as 9 MHz, but intensity is systematically reduced with increasing C_q. We have derived new data for isotropic chemical shifts for five or six of the eight sites in crystalline anorthite, which agree reasonably well with previous correlations with structure. In glasses, the separation between peaks for Al in different coordination states is excellent, and provides a new and sensitive test for the presence of AlO_5 and AlO_6 sites in glasses dominated by AlO_4, although absolute quantitation may remain difficult.

Acknowledgment. We thank Jane Oglesby and Jed Mosenfelder for providing glass samples and P. J. Grandinetti for a preprint describing new 3QMAS experiments[2] and useful discussions on the experimental setup and data analysis. A.P. also acknowledges support from Otsuka Electronics/Chemagnetics. This work was funded by the National Science Foundation, Grant Nos. EAR9204458 and EAR9506393, and the Director of the Office of Energy Research, Office of Basic Energy Sciences, Materials Sciences Division of the U.S. Department of Energy under Contract No. DE-AC03-76SF00098. J.H.B. was partially supported by a Camille and Henry Dreyfus startup grant and a Research Corporation Cottrell College Grant.

Supporting Information Available: The 2D triple-quantum ^{27}Al MAS NMR spectrum of crystalline anorthite collected at 9.4 T (1 page). See any current masthead page for ordering and Internet access instructions.

JA9606586